catalysts

MDPI

Article

Catalytic Partial Oxidation of Methane to Methanol over Fe_2O_3/MWCNTs

Zhengqing Zhou [1,*], Yinghua Zhang [1], Zhian Huang [1], Jia Liu [1], Jinguo Sang [2], Zuochun Luan [3], Wei Tian [2], Yukun Gao [1], Xingyu Zhang [1], Yucheng Ji [1] and Tao Tang [1]

[1] School of Civil and Resource Engineering, University of Science and Technology, Beijing 100083, China; gaoyukunustb@sina.com (Y.G.); tangtao@ustb.edu.cn (T.T.)
[2] Shandong Goldsoft Technology Co., Ltd., Zhaoyuan 265400, China
[3] Shandong Guohuan Solid Waste Innovation and Technology Center Co., Ltd., Zhaoyuan 265400, China
* Correspondence: zhouzhengqing2016@163.com or zhouzhengqing@ustb.edu.cn

Abstract: The catalytic partial oxidation of methane (CPOM) to methanol has been regarded as a promising approach for methane utilization, despite that the conversion remains a formidable challenge in the perspective of catalysts. A novel catalyst system of multi-wall carbon nanotubes (MWCNTs) that supported Fe_2O_3 with existing I_2, consisting of non-noble metal and working in weak acid at an ambient temperature, was investigated for CPOM. MWCNTs supported the Fe_2O_3 catalyst, which was prepared by the impregnation method and characterized via HRTEM, XRD, XPS, FT-IR, and BET techniques. The characterization results reveal that, as a non-noble metal catalyst, the Fe_2O_3/MWCNTs catalyst had a good catalytic performance and stability in the CPOM. With the variation of reaction pressure and the dosage of Fe_2O_3/MWCNTs, the catalyst system obtained the highest methane conversion rate of 7.41% and methanol selectivity of 86.3%, which is analogous to that of the equivalently strong acid catalyst system. The I_2-Fe_2O_3/MWCNTs catalyst system has great potential in the application of CPOM under mild, environmentally benign conditions, such as non-noble metal requirement, ambient temperature, and weak acid. The reaction mechanism was discussed.

Keywords: partial oxidation; carbon nanotubes; weak acid; non-noble metal

Citation: Zhou, Z.; Zhang, Y.; Huang, Z.; Liu, J.; Sang, J.; Luan, Z.; Tian, W.; Gao, Y.; Zhang, X.; Ji, Y.; et al. Catalytic Partial Oxidation of Methane to Methanol over Fe_2O_3/MWCNTs. *Catalysts* **2024**, *14*, 134. https://doi.org/10.3390/catal14020134

Academic Editor: Leonarda Liotta

Received: 2 January 2024
Revised: 25 January 2024
Accepted: 26 January 2024
Published: 8 February 2024

Correction Statement: This article has been republished with a minor change. The change does not affect the scientific content of the article and further details are available within the backmatter of the website version of this article.

1. Introduction

Methane serves as a valuable fuel resource and ranks as the second most abundant greenhouse gas after carbon dioxide [1]. The use of the catalytic partial oxidation of methane (CPOM) for resource-oriented utilization not only mitigates methane emissions, but also generates chemical raw materials for the chemical industry. Additionally, it produces a highly energy-dense liquid fuel that can be efficiently transported and stored over long distances. Due to its inherent advantages and potential, CPOM has emerged as the most promising method for the resource-oriented utilization of methane, attracting global attention from researchers [2–6].

A primary challenge in the CPOM process is the activation of the methane C–H bond and the preservation and isolation of intermediate products [7]. Numerous studies have diligently sought optimal solutions to overcome these challenges. Lance and Elworthy reported the method for synthesizing methanol through the oxidation of methane with hydrogen peroxide in the presence of ferrous sulfate [8]. Periana et al. achieved the synthesis of methanol derivatives from methane by employing methyl bisulfate and a mercuric bisulfate catalyst [9]. Subsequently, molybdenum-based and vanadium-based materials emerged as highly efficient catalysts, exhibiting excellent oxidation activity and selectivity for methane. However, these catalysts still relied on noble metals, and noble metal catalysts have consistently faced challenges when it comes to their separation from the final product [10,11]. Additionally, noble metal catalysts often carry a high cost that

renders them unsuitable for widespread commercial application. Moreover, these catalyst systems involve the use of highly dangerous and corrosive strong acid solvents, imposing stringent demands on the equipment and its maintenance.

Since then, significant efforts have been made to address the challenges associated with the presence of strong acidic solutions and noble metals in conventional catalyst systems [12,13]. Chen et al. [14] conducted catalytic oxidation experiments in which they utilized heteropoly acid, known for its strong oxidizing properties, to enhance the polar nature of acetic acid, effectively replacing strong acid systems like fuming sulfuric acid and trifluoroacetic acid. Zhang et al. investigated the influence of glacial acetic acid and heteropoly acid on the CPOM process, discovering that increasing the acidity of -COOH and the concentration of glacial acetic acid resulted in a moderate promotion of the catalytic oxidation of methane.

Monooxygenase, found in nature, has the ability to selectively convert methane into methanol under mild conditions. It has led to the development of a new branch in catalysts and made it possible to replace noble metals in catalyst compounds. The paradigm shift resulted from the discovery that zeolites, such as ZSM-5 and mordenite, can stabilize binuclear iron [15,16] and copper centers [17,18]. Fe-ZSM-5 can convert methane into methanol at room temperature. Iron-containing zeolites, including iron sodalite, exhibited a 70% selectivity for methanol at 5.7% methane conversion at 689 K. The reports by Michalkiewicz et al. presented the impressive activity of an iodine-containing compound catalyst in the CPOM process. Elemental iodine dissolved in weak oleum catalyzed the functionalization of methane to methyl bisulfate with a concentration of 45% and a selectivity of over 90% [19]. The discovery prompted the examination of other halogen compounds in oleum. The discovery revealed that iodine-based catalysts have the potential to replace noble metal catalysts.

In recent years, researchers have utilized carbon nanotubes (CNTs) as a supporting material to enhance the catalytic efficiency in the development of novel catalysts. Xie et al. [20] investigated the effects of CNTs on the catalytic properties of CeO_2/xCNTs-CuO and found that the presence of CNTs significantly increased the number of active centers and the concentration of oxygen vacancies in CeO_2/xCNTs-CuO, leading to improved catalytic performance and enhanced resistance to oxidation. Shi et al. [21] examined the preferential oxidation of CO over CuO/CeO_2 catalysts confined by carbon nanotubes and discovered that the confinement of carbon nanotubes greatly enhanced the reduction of active copper. Wei et al. [22] reported that the confinement of iron oxides within CNTs enhanced their redox properties, resulting in a more reduced state during Fischer–Tropsch synthesis. Furthermore, the size of the iron oxide particles remained consistent before and after the reaction, indicating that particle sintering was prevented due to the spatial restriction provided by CNTs. The unique structure and properties of CNTs allow for a remarkable improvement in the reaction efficiency of the encapsulated materials [23]. Consequently, CNTs are widely utilized as a support medium for catalyst development [24–26].

A novel and green catalyst system for CPOM was built up, which was applied under a mild condition. In the glacial acetic acid, the Fe_2O_3/MWCNTS catalyst system with existing I_2 was established to catalyze methane. The crystal structure, micro-morphology, chemical composition, and catalysis performance of as-prepared Fe_2O_3/MWCNTS were characterized by using various analysis techniques. Then, the parameter optimization and stability of the Fe_2O_3/MWCNTs catalyst system was investigated. Finally, on the basis of the above, the mechanism of the conversion of methane to methanol by the Fe_2O_3/MWCNTS catalyst system with existing I_2 is proposed. The present work provides significant guidance to construct the mild photocatalytic system toward the selective conversion of methane.

2. Results and Discussion

2.1. Analysis of Fe_2O_3/MWCNTs Characterization Experiments

2.1.1. Morphology

The TEM images of Fe_2O_3/MWCNTs are shown in Figure 1. It can be seen from Figure 1a,b that the Fe_2O_3 nano particles (NPs) are uniformly loaded on the surface and encapsulated inside the MWCNTs. Approximately 80% of the particles fall in the range of 5–15 nm (Figure 1d). The HRTEM image (Figure 1c) reveals that a lattice space of 0.25 nm corresponds to the (110) crystal face of Fe_2O_3, indicating the presence of more active oxygen species, which is beneficial for higher catalytic activities [27].

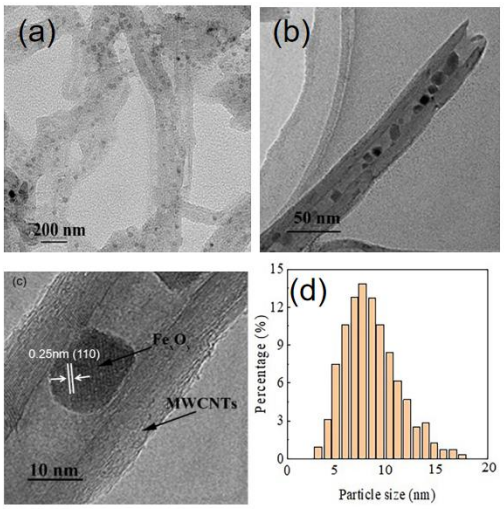

Figure 1. TEM images (**a**,**b**), HRTEM image (**c**), and particle size (**d**) of Fe_2O_3/MWCNTs.

2.1.2. Crystalline Structure

Figure 2 shows the XRD spectra of Fe_2O_3/MWCNTs catalysts. As shown in Figure 3, there is a significant characteristic diffraction peak of carbon nanotubes at $2\theta = 26.6^\circ$ for the Fe_2O_3/MWCNTs samples, corresponding to the (002) crystal face of carbon nanotubes. The peak positions and intensity are consistent with the standard values of the α-Fe_2O_3 of the standard JCPDS (NO. 33–0664), corresponding to the main characteristic diffraction peaks of the (012), (104), (110), (113), (024), (116), (214), and (300) crystal face of α-Fe_2O_3, respectively. Among them, the strong signal of $2\theta = 35.8^\circ$ corresponding to the (110) crystal face is generally consistent with the observation of HRTEM.

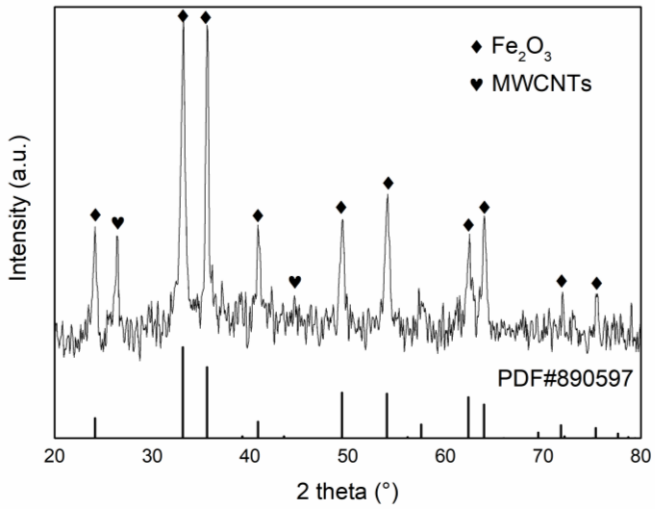

Figure 2. XRD patterns of Fe_2O_3/MWCNTs.

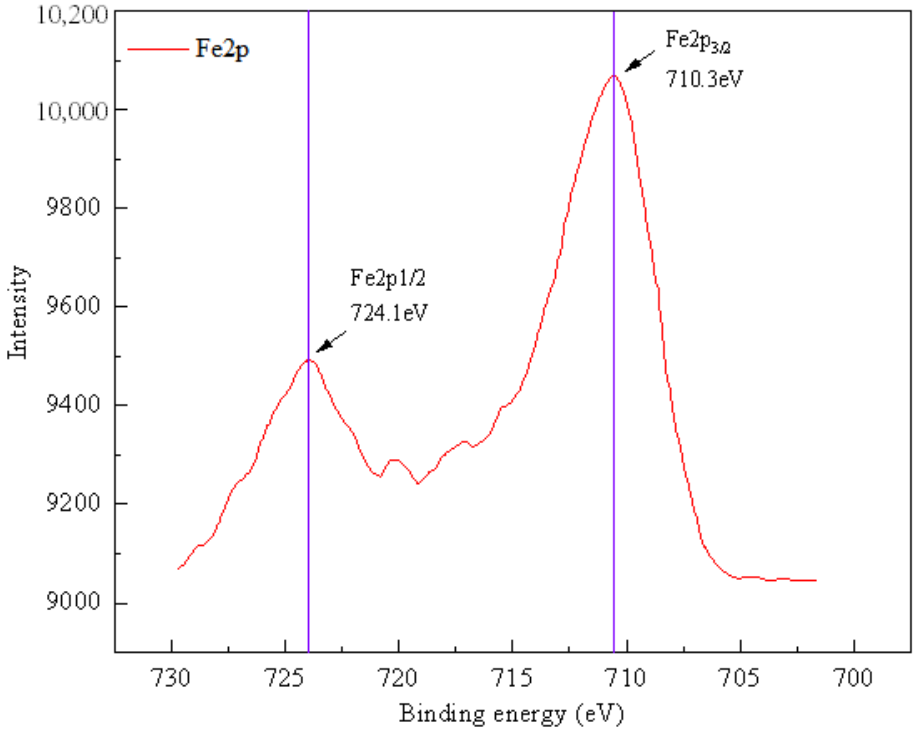

Figure 3. XPS spectra of Fe for Fe_2O_3/MWCNTs prepared by impregnation method.

2.1.3. XPS Analysis

In order to determine the chemical form of Fe in the compound formed on the surface of MWCNTs, XPS tests are performed on the Fe_2O_3/MWCNTs catalyst. The XPS spectra of Fe are shown in Figure 3. The 2p orbital of the Fe element is divided into two electron orbitals of Fe2p1/2 and Fe2p3/2. Their electron binding energies are 724.1 eV and 710.3 eV, respectively, both of which are characteristic peaks of Fe^{3+}. It demonstrates that, for the Fe_2O_3/MWCNTs catalyst, the Fe-based component exists in the form of Fe_2O_3 on the surface or within the pore structure of MWCNTs [19].

2.1.4. FT-IR Analysis

Figure 4 shows the FT-IR spectra of pure MWCNTs and Fe_2O_3/MWCNTs. By comparing the infrared spectra of pure MWCNTs and Fe_2O_3/MWCNTs in Figure 4, it can be observed that a strong absorption peak appears at 1720 cm^{-1}, which corresponds to the C=O stretching vibration peak of (-COOH). The intensity of the C=O stretching vibration peak abates after the MWCNTs in the Fe_2O_3/MWCNTs complete the load of Fe_2O_3. And a new characteristic absorption peak emerges between 550 cm^{-1} and 700 cm^{-1}, while the Fe–O characteristic absorption peak of Fe_2O_3 has characteristics of a contraction vibration peak at 569 cm^{-1}. Therefore, the new characteristic peak between 700 cm^{-1} and 550 cm^{-1} should be a Fe–O contraction vibration peak. The peak value shifts slightly, which is due to the effects of complex chemical bonding which generate in the formation of the compounds on the surface of MWCNTs. It indicates that the process of loading iron onto MWCNTs involves the iron and carboxyl groups on the carbon nanotubes reacting and forming new Fe–O bonds, resulting in the consumption of hydroxyl groups. The entire process of iron-loaded carbon nanotubes is shown in Figure 5.

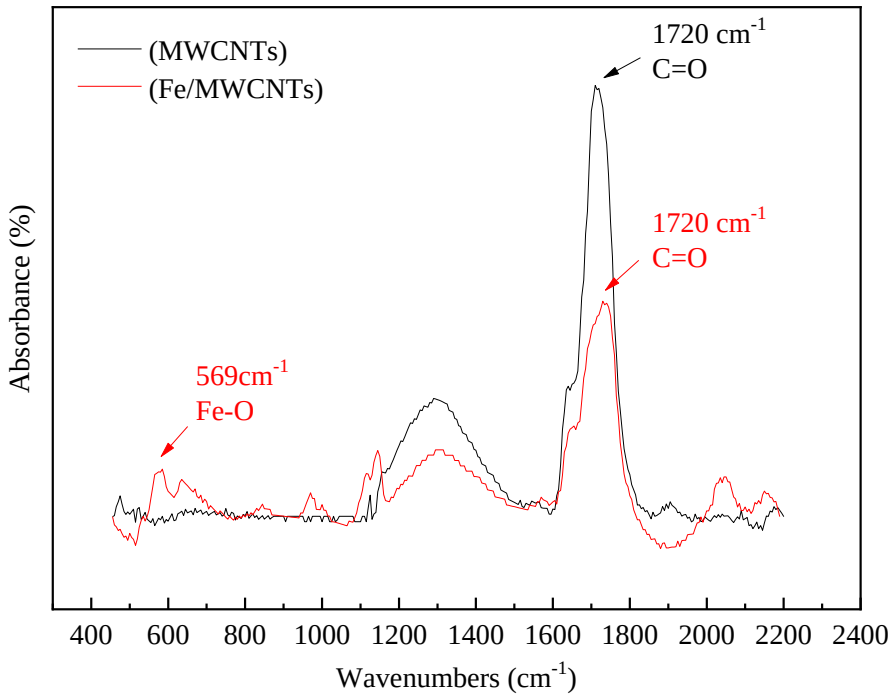

Figure 4. FT-IR spectra of MWCNTs and Fe_2O_3/MWCNTs.

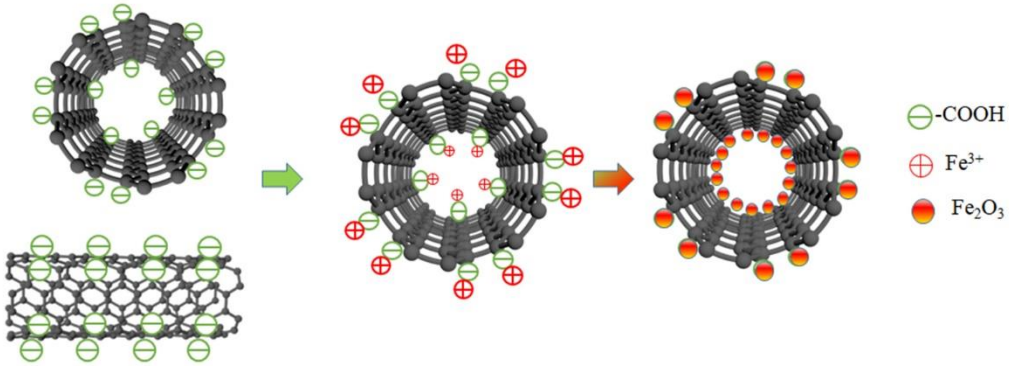

Figure 5. The schematic diagram of the process of MWCNTs supporting Fe_2O_3.

2.1.5. Textural Properties Analysis

Table 1 shows the data of the specific surface area, pore volume, and pore diameter of pure Fe_2O_3, pure MWCNTs, and Fe_2O_3/MWCNTs. As can be seen in Table 1, the specific surface area of pure Fe_2O_3 is 32.83 m^2/g. However, it is 168.82 m^2/g for that of Fe_2O_3/MWCNTs, which is five times larger than that of pure Fe_2O_3. Compared with the pure MWCNTS, the specific surface area of Fe_2O_3/MWCNTS increases to some extent, but the pore volume and pore diameter decrease significantly. The increase in the specific surface areas can be attributed to the iron, which is encapsulated within the pore channels of MWCNTs, occupies part of the pore space, forms highly dispersed Fe-based nanoparticles, and causes more intergranular pores. Therefore, the confinement of carbon nanotubes benefits the active component of Fe_2O_3 because of more dispersal, which is more favorable for the contact between Fe_2O_3 and the reactants since it increases the reaction contact surface and boosts the reaction efficiency.

Table 1. Textural properties of MWCNTs, Fe_2O_3/MWCNTs, Fe_2O_3.

Samples	S_{BET} [a] (m^2/g)	V_{BJH} [b] (cm^3/g)	D_{pore} [c] (nm)
Pure Fe_2O_3	32.83	0.21	3.89
Pure MWCNTs	152.48	1.95	52.67
Fe_2O_3/MWCNTs [d]	168.82	0.52	10.28

[a] S_{BET} denotes the BET surface area. [b] V_{BJH} represents the pore volume evaluated by the BJH method. [c] D_{pore} denotes the average pore diameter. [d] Represents Fe_2O_3/MWCNTs.

2.2. Parameter Optimization and Stability of the Fe_2O_3/MWCNTs Catalyst System

2.2.1. Effects of the Pressure of the Fe_2O_3/MWCNTs Catalyst System on the CPOM

Figure 6 shows the changes in the methane conversion rate, methanol concentration, and CH_3OH selectivity with the variation of methane gas pressure in the CPOM. As shown in Figure 6, the concentration of methanol increases with the pressure of the methane reaction increasing. At the reaction pressures of 3 MPa and 4 MPa, the methanol concentrations are 358.37 ppm and 392.88 ppm, respectively. When the methane pressure rises to 4 MPa, the growth of methanol concentrations slows down as the methane pressure increases. It indicates that when the methane pressure reaches 4 MPa, the reactive center provided by the catalyst has been surrounded by enough methane molecules. When the pressure of methane continues to increase, the extra methane molecules cannot come in contact with the reactive center. At a pressure of 3 MPa, the methane conversion rate is 6.56%; when the pressure is between 3 MPa and 4 MPa, the conversion curve is flat. When it exceeds 4 MPa, the conversion rate starts to rise up again, while CH_3OH selectivity decreases from 81% to 74%. The reason for the conversion's increase is that after the CH_3OH concentration reaches the threshold value at 3 MPa, the continuous additional pressure leads to the emergence of side-products of CPOM. This is also testified by the result of the products' test in the gas phase, in which the concentration of CO_2, and the production of the deep oxidation of methane, increased by approximately 10% along with the pressure increasing from 3 MPa to 5 MPa. Taking the balance between the methane conversion rate and methanol concentrations into consideration, the following experiment will set the pressure to 3 MPa.

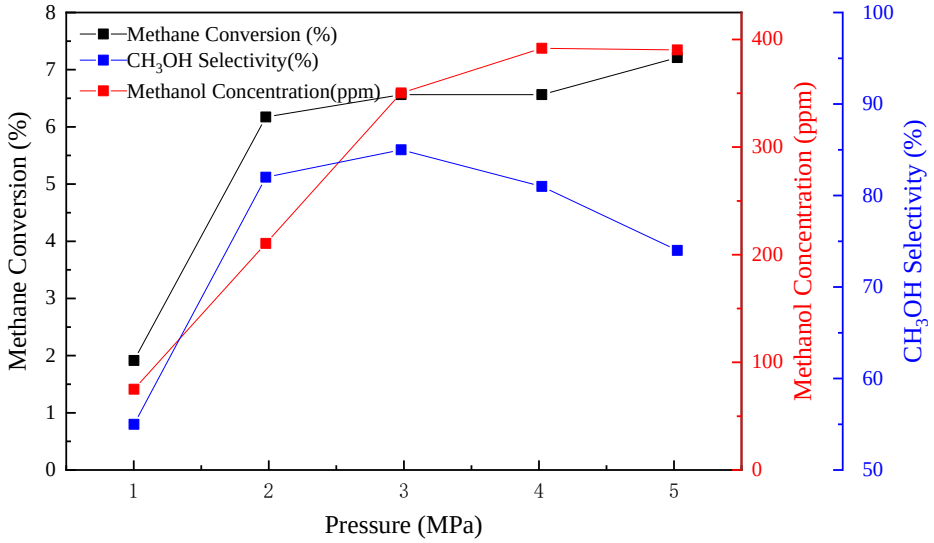

Figure 6. Effects of pressure on methane conversion in the CPOM (temperature 30 °C, iron loading of Fe_2O_3/MWCNTs 45%, glacial acetic acid solution 100 mL, iodine concentration 0.035 mol/L, the catalyst dosage 0.1 g).

2.2.2. Effects of the Fe_2O_3/MWCNTs Dosage of the Fe_2O_3/MWCNTs Catalyst System on the CPOM

Figure 7 shows the effects of the Fe_2O_3/MWCNTs dosage of the Fe_2O_3/MWCNTs catalyst system on the CPOM. It can be seen from Figure 8 that the methane conversion rate and the methanol concentration have a positive correlation with the Fe_2O_3/MWCNTs dosage. Much more methane molecules can participate in the CPOM due to the increase in the catalyst dosage, which provides more active centers, which is beneficial to the methane conversion; CH_3OH selectivity is improved significantly by the addition of Fe_2O_3/MWCNTs, and its curve increases sharply when Fe_2O_3/MWCNTs were added. However, when the catalyst dosage exceeds 0.15 g/100 mL, the methane conversion and methanol concentration exhibit a stable trend as well as CH_3OH selectivity. When the dosage of Fe_2O_3/MWCNTs in 100 mL of iodine solution (0.035 M) is 0.15 g, the maximum concentration of methanol reaches 363.55 ppm, the methane conversion is 7.41%, and the CH_3OH selectivity is above 80%. Therefore, the optimum catalyst dosage obtained under the experimental condition is 0.15 g/100 mL.

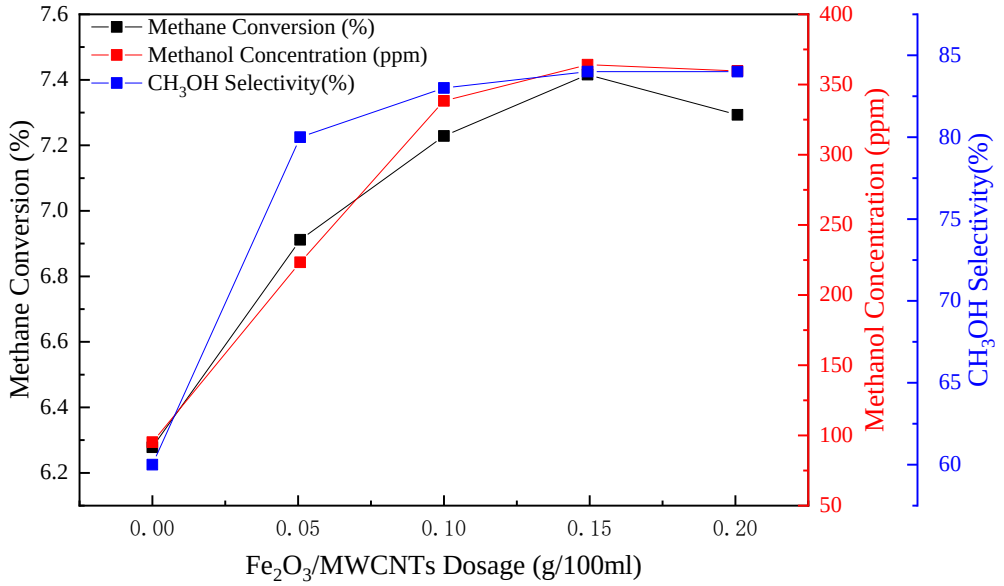

Figure 7. Effects of the dosage of Fe_2O_3/MWCNTs on methane conversion in the CPOM (temperature 30 °C, pressure 3 MPa, iron loading of Fe_2O_3/MWCNTs 45%, glacial acetic acid solution 100 mL, iodine concentration 0.035 mol/L).

The literature [28,29] reported that the conversion rate of methane could be remarkably increased by directly increasing the acidity of the reaction solution, such as the addition of heteropoly acids. But its drawback is that it is environmentally unfriendly and puts forward a higher requirement for experimental equipment. Compared with the reaction system catalyzed by iodine alone [16], the addition of Fe_2O_3/MWCNTs can effectively improve the conversion of methane. The methane conversion rate increases from 6.28% to 7.41%, and the methanol concentration increases from 99.45 ppm to 363.55 ppm. The experimental results indicate that the efficiency of CPOM over Fe_2O_3/MWCNTS catalysts with existing I_2 is close to that of adding heteropoly acids. Likewise, CPOM over the I_2-Fe_2O_3/MWCNTS catalyst system is environmentally friendly, which has less damage to the instrument and can meet the requirements of green environmental protection.

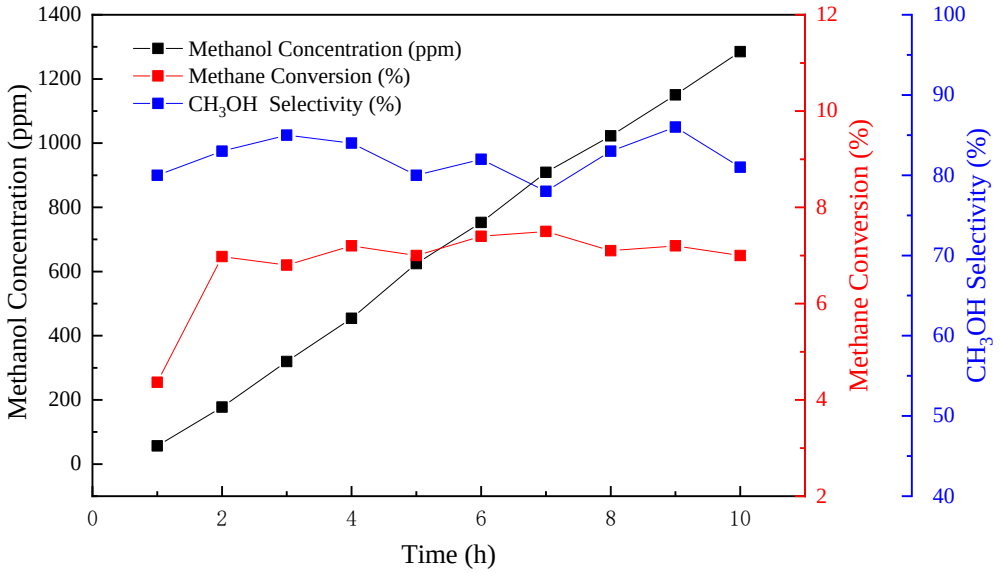

Figure 8. Stability analysis of methane conversion, CH_3OH selectivity, and methanol concentration over a 10-h continuous period of assessment.

2.2.3. Stability Analysis of Fe_2O_3/MWCNTs Catalyst System on the CPOM

After the optimized parameters were obtained, the Fe_2O_3/MWCNTs catalyst system with existing I_2 was assessed for its stability over 10 h of continuous CPOM operation. The stability test was carried out under the pressure of 3 MPa, the catalyst dosage was 0.15 g/100 mL, the reaction temperature was 30 °C, and the iodine concentration was 0.035 mol/L.

As shown in Figure 8, the curve of the yields of methanol from 2 h to 10 h tends to be linear. The methane conversion rises up from 4.37% to 6.98%. After 2 h reaction time, the conversion rate waves up and down at the level of 7%. CH_3OH selectivity fluctuates slightly, but stays above 80% basically and reaches for the highest of 86.3%. It indicates that when the reaction time exceeds 2 h, methanol's yield in each hour is flat, and the methane conversion starts to be stable, while the selectivity holds steady at more than 80%. Based on the analysis of the results of 10 h of continuous CPOM operation, the changes in the three indexes demonstrate that the Fe_2O_3/MWCNTs catalyst system presents good stability to deactivation and poisoning by reaction products. The reason for this is that the lower reaction temperature of the novel catalytic system avoids high-temperature sintering, which always causes the deactivation of the catalyst system. Likewise, the confinement effects and excellent conductivity of MWCNTs accelerate the transaction process and weaken the possibility of coking and poisoning by products.

2.3. Catalytic Mechanism Analysis of CPOM over I_2-Fe_2O_3/MWCNTs

Iron plays a crucial role in the activation of C–H bonds. The formation of α-Fe_2O_3 on the surface of MWCNTs is critical in enhancing the catalytic efficiency of the CPOM process during the catalytic oxidation of methane. The tubular and porous structure of MWCNTs positively impacts the catalytic efficiency. The confinement effect of MWCNTs facilitates increased contact between methane molecules and the active centers within a limited space. Additionally, the confinement within the MWCNTs can also enhance the redox properties of encapsulated iron oxides, resulting in a more reduced state of the iron species inside the MWCNT channels [30]. The uniform pore diameter in this structure ensures consistent contact between the catalyst surface and methane molecules. Furthermore, the MWCNTs' support facilitates the high dispersion of α-Fe_2O_3 within the finite tube-pore structure, leading to a significant increase in the surface area. These characteristics collectively contribute to the promotion of the catalytic efficiency of the I_2-Fe_2O_3/MWCNTs catalyst system.

α-Fe_2O_3 nanocrystals with more reactive crystal faces (110) have a higher activity than the other samples. The (110) crystal face, with a relative higher density of Fe atoms, exhibits a higher activity than other Fe species [26]. Meanwhile, the irregular arrangement of atoms in the deformation boundary layer and chaotic zone can be observed at the junction of the main crystal face. In these areas, Fe and O atoms cannot be arranged in accordance with the original α-Fe_2O_3 crystal phase lattice, causing vacancy defects, inversion defects, dislocation, grain boundary and topological defects, and other defects. It has been reported in the literatures that these special structures and defects of the α-Fe_2O_3 crystal face have strong adsorption capacity for oxygen species, which contributes to improving the active adsorption of oxides and the excellent catalytic activation of the methane C–H bond [31]. Both of the highly active crystal faces and special defect structures enhance the activity of the reaction center of Fe_2O_3/MWCNTs and improve its catalytic performance to methane molecules.

In the catalytic routine shown in Figure 9, the acidic medium ice acetic acid plays a very crucial role in the catalytic cycle process. The acidity of the glacial acetic acid system is favorable for the electron donating tendency of methane and the electrophilic activation of the methane molecule. Meanwhile, glacial acetic acid, as a nucleophile, can replace the methane intermediate CH_3IH^+ to produce methyl acetate, which can avoid deep oxidation and improve the methanol product selectivity. Iodine is one of the most actively non-metallic catalyst with the properties of transition-metal under high pressure, and the catalytic process of methane in acetic acid solvent by iodine can be considered to belong to an electrophilic displacement mechanism [32]. In acetic acid solvent, iodine is firstly oxidized to active I^+, which then electrophilically attacks methane to produce the intermediate CH_3IH^+. The acetic acid acts as the nucleophile to react with the intermediate CH_3IH^+ to produce esterification. Subsequently, methanol was formed as a result of ester hydrolysis. The selective oxidation of methane to methanol can be represented by the following equation [33]:

$$CH_4 + I^+ \rightarrow CH_3IH^+ \quad (1)$$

$$CH_3IH^+ + CH_3COOH \rightarrow CH_3COOCH_3 + HI + H^+ \quad (2)$$

$$HI + H^+ + CH_3COOCH_3 + H_2O \rightarrow CH_3OH + CH_3COOH + I^+ \quad (3)$$

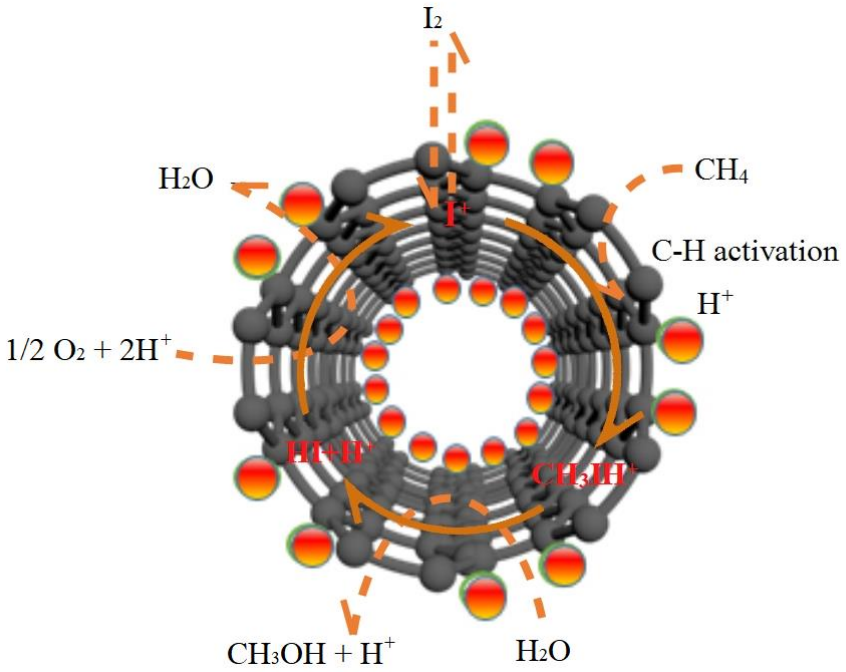

Figure 9. Diagram of catalytic routine of CPOM over I_2-Fe_2O_3/MWCNTs in the glacial acetic acid.

3. Experiments

3.1. Preparation of Fe_2O_3/MWCNTs Catalysts

The Fe_2O_3/MWCNTs catalyst was synthesized by the impregnation method. A certain amount of $Fe(NO_3)_3 \cdot 9H_2O$ was firstly weighed and mixed with anhydrous ethanol, followed by MWCNTs (OD:10–20 nm, purchased from Shanghai pioneer nano Co., Ltd., Shanghai, China), which were added and stirred evenly. Afterwards, the mixture was dried thoroughly in the oven at 105 °C to ensure complete volatilization. Once dried, the mixture was grinded to obtain the black compound. Finally, the compound was sintered in the muffle furnace at 350 °C for 2 h to obtain the sample.

3.2. Characterization of Catalysts

The morphology of the catalyst was obtained using the Tecnai G2 F20 transmission electron microscope (TEM, Hillsboro, OR, USA). With the 3H-2000PS2 specific surface area and pore diameter analyzer (Beijing, China), the BET specific surface area, BJH pore distribution, and pore volume of Fe_2O_3/MWCNTs was determined. The crystal lattice structure and crystal morphology of the catalyst was measured using an X-ray diffractometer with a graphite monochromator and Cu Kα radiation (Bruker Corporation, Ltd., Karlsruher, Germany). XPS was performed on an ESCALAB250XI spectrometer (Waltham, MA, USA) with the monochromatized Al-Kα X-ray source to determine the oxidation states of the metals. FT-IR analysis was conducted with an Affinity-1S Fourier transform infrared spectrometer (Shimadzu Corporation, Ltd., Kyoto, Japan).

3.3. CPOM in the Liquid Phase

1. Ball valve, 2. pressure gauge, 3. pressure regulator, 4. filter, 5. shut-off valve, 6. mass flow meter, 7. check valve, 8. three-way valve, 9. heating and stirring switch, 10. speed display panel, 11. speed adjustment knob, 12. reaction kettle temperature display, 13. reaction kettle set temperature, 14. temperature setting button, 15. intake tube, 16. exhaust tube, 17. temperature sensor, 18. magnetic stirrer, 19. back pressure valve, 20. reaction kettle, 21. safety valve. The CPOM in the liquid phase was carried out using an SLM500 micro high-pressure reactor. The setup for the lab experiments is shown in Figure 10. The detailed steps for operation were as follows: 100 mL of glacial acetic acid solution and a certain amount of catalyst were taken to prepare a mixed solution. Next, the mixed solution was transferred into the quartz lining of the reactor, and a magnetic agitator was put into the solution. Then, the reactor was sealed. After the air tightness was confirmed to meet the requirement, the air in the device was discharged and methane gas was filled up to reach a certain pressure. The experimental preparation was completed while the pressure in the device achieved the set value. The reaction kettle and timing started. Heating and stirring stopped when the reaction time of 2 h ran out. The reaction pressures were set at 1 MPa, 2 MPa, 3 MPa, 4 MPa, and 5 MPa, respectively, while the reaction temperature was 30 °C, the iron loading of Fe_2O_3/MWCNTs was 45%, the glacial acetic acid solution was 100 mL, the iodine concentration was 0.035 mol/L, the catalyst dosage was 0.1 g, the reaction time was 3 h, and the stirring rate was 500 rpm. Analogously for the effects of catalyst dosage, experiments were carried out while the catalyst dosage stepwise varied from 0.05 g to 0.20 g at a 0.05 g step with a certain pressure confirmed by the former experiments. The gas before and after the reaction was detected via the gas chromatography technique with an Agilent 6820 gas chromatograph (Agilent Technologies Corporation, Ltd., Palo Alto, Santa Clara, CA, USA). The products in the liquid phase were determined and qualitatively analyzed via the gas chromatography-mass spectrometry technique with a Shimadzu-QP2010-ultra GC-MS (Shimadzu Corporation, Ltd., Kyoto, Japan).

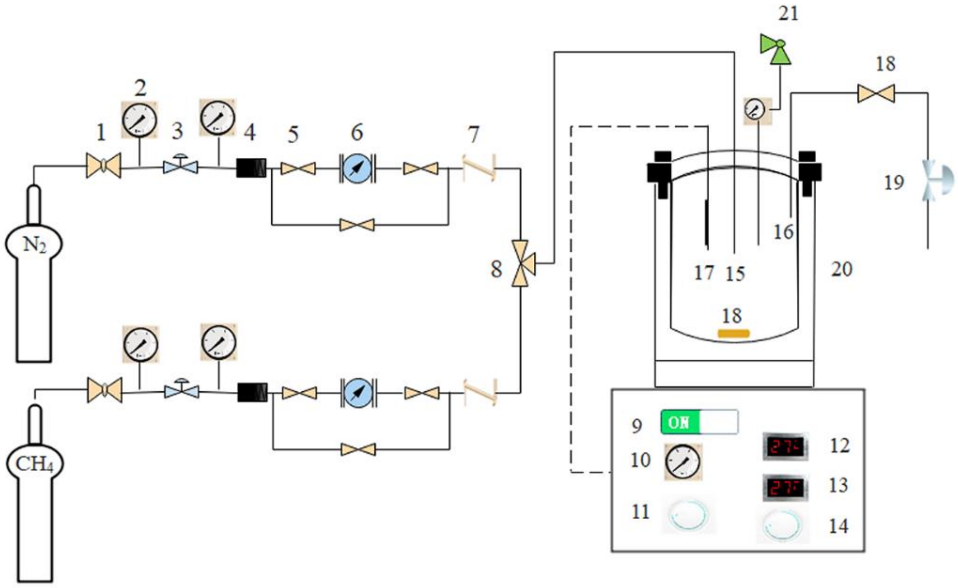

Figure 10. Schematic of CPOM setup in the liquid phase.

4. Conclusions

(1) A novel and green catalyst system for the CPOM was built up, which was applied under a mild condition. In the glacial acetic acid, the Fe_2O_3/MWCNTS catalyst system with existing I_2 was established to catalyze methane, and the methane conversion rate and concentrations of methanol were close to that of an equivalently strong acid system. And its catalytic mechanism and reaction path were theoretically analyzed. Compared with conventional catalyst systems, the novel catalyst system did not involve strong acids, noble metals, or other additives, which had a lower requirement for experimental equipment and maintenance, and was environmentally friendly at an affordable cost.

(2) The characterization results of Fe_2O_3/MWCNTs by BET, XRD, HRTEM, XPS, and FT-IR indicate that the catalyst of Fe_2O_3/MWCNTs exhibits effective particle adhesion, uniform dispersion, and the avoidance of agglomeration. The specific surface area of Fe_2O_3/MWCNTs prepared by the impregnation method is 168.82 m^2/g, which is five times larger than that of pure Fe_2O_3 (32.83 m^2/g). MWCNTs, as a support, retain the original structure during the formation of Fe_2O_3/MWCNTs. The active catalytic component generated on MWCNTs is mainly α-Fe_2O_3, which is evenly dispersed on the surface of the carrier and forms (110) crystal faces with high activity for methane oxidation. The tube-pore structure of WMCNTs not only significantly increases the specific surface area of the catalyst particles after loading, but also increases the contacts between the methane molecules and activation centers in a limited space due to the confinement effect of the tube-pore structure.

(3) Experiments on the reaction pressure and dosage of Fe_2O_3/MWCNTs in the CPOM show that when the pressure is 3 MPa, the catalyst dosage is 0.15 g/100 mL, the reaction temperature is 30 °C, the iodine concentration is 0.035 mol/L, and the methanol selectivity reaches the highest value of 86.3%. The results of the stability test show that the changes in methane conversion, methanol concentration, and CH_3OH selectivity testify to the excellent stability of the Fe_2O_3/MWCNTs catalyst system to deactivation and poisoning by reaction products over the 10 h continuous CPOM operation.

Author Contributions: Conceptualization, J.L., Y.Z. and Z.Z.; methodology, J.L. and Y.J.; validation, W.T.; formal analysis, Z.H., Y.G. and J.L.; investigation, Z.Z. and X.Z.; resources, J.S., J.L. and Z.L.; data curation, Y.J. and J.L.; writing—original draft preparation, Y.J. and T.T.; writing—review and editing, Y.J., Y.Z., Z.H. and Y.G.; visualization, Y.J. and T.T.; supervision, Y.Z. and Z.H.; project administration, Y.G.; funding acquisition, Y.Z. and Z.H.; All authors have read and agreed to the published version of the manuscript.

Funding: This research was funded by Fundamental Research Funds for the Central Universities: FRF-TP-20-005A1; Shandong Province Science and Technology-Based Small and Medium-sized Enterprise Innovation Capability Enhancement Project: 2023TSGC0845; National Key R&D Program of China: 2023YFC3009800.

Data Availability Statement: The data presented in this study are available.

Conflicts of Interest: Jinguo Sang and Wei Tian were employed by the company Shandong Jinruan Science and Technology Co., Ltd. Zuochun Luan was employed by the company Shandong Guohuan Solid Waste Innovation and Technology Center Co., Ltd. The remaining authors declare that the research was conducted in the absence of any commercial or financial relationships that could be construed as a potential conflict of interest.

References

1. Zakaria, Z.; Kamarudin, S. Direct conversion technologies of methane to methanol: An overview. *Renew. Sustain. Energy Rev.* **2016**, *65*, 250–261. [CrossRef]
2. Mansouri, S.; Benlounes, O.; Rabia, C.; Thouvenot, R.; Bettahar, M.; Hocine, S. Partial oxidation of methane over modified Keggin-type polyoxotungstates. *J. Mol. Catal. A Chem.* **2013**, *379*, 255–262. [CrossRef]
3. Ferreira, A.C.; Ferraria, A.; Rego, A.B.D.; Gonçalves, A.P.; Girão, A.V.; Correia, R.; Gasche, T.A.; Branco, J.B. Partial oxidation of methane over bimetallic copper–cerium oxide catalysts. *J. Mol. Catal. A Chem.* **2010**, *320*, 47–55. [CrossRef]
4. Chawdhury, P.; Kumar, D.; Subrahmanyam, C. NTP reactor for a single stage methane conversion to methanol: Influence of catalyst addition and effect of promoters. *Chem. Eng. J.* **2019**, *372*, 638–647. [CrossRef]
5. Raynes, S.; Shah, M.A.; Taylor, R.A. Direct conversion of methane to methanol with zeolites: Towards understanding the role of extra-framework d-block metal and zeolite framework type. *Dalton Trans.* **2019**, *48*, 10364–10384. [CrossRef] [PubMed]
6. Dinh, K.T.; Sullivan, M.M.; Narsimhan, K.; Serna, P.; Meyer, R.J.; Dincă, M.; Román-Leshkov, Y. Continuous partial oxidation of methane to methanol catalyzed by diffusion-paired copper dimers in copper-exchanged zeo-lites. *J. Am. Chem. Soc.* **2019**, *141*, 11641–11650. [CrossRef] [PubMed]
7. Park, K.-W.; Seo, H.J.; Kwon, O.-Y. Mesoporous silica-pillared titanosilicate as catalytic support for partial oxidation of methane. *Microporous Mesoporous Mater.* **2014**, *195*, 191–196. [CrossRef]
8. Xie, J.; Jin, R.; Li, A.; Bi, Y.; Ruan, Q.; Deng, Y.; Zhang, Y.; Yao, S.; Sankar, G.; Ma, D.; et al. Highly selective oxidation of methane to methanol at ambient conditions by titanium dioxide-supported iron species. *Nat. Catal.* **2018**, *1*, 889–896. [CrossRef]
9. Ravi, M.; Ranocchiari, M.; van Bokhoven, J.A. The direct catalytic oxidation of methane to methanol-A critical assessment. *Angew. Chem. Int. Ed.* **2017**, *56*, 16464–16483. [CrossRef]
10. Hannemann, S.; Grunwaldt, J.-D.; Lienemann, P.; Günther, D.; Krumeich, F.; Pratsinis, S.E.; Baiker, A. Combination of flame synthesis and high-throughput experimentation: The preparation of alumina-supported noble metal particles and their application in the partial oxidation of methane. *Appl. Catal. A Gen.* **2007**, *316*, 226–239. [CrossRef]
11. András, G.; Rajkumar, M.; Ábel, A.; Efremova, A. Noble-metal-free and Pt nanoparticles-loaded, mesoporous oxides as efficient catalysts for CO_2 hydrogenation and dry reforming with methane. *J. CO_2 Util.* **2019**, *32*, 106–118. [CrossRef]
12. Sun, M.; Zhang, J.; Putaj, P.; Caps, V.; Lefebvre, F.; Pelletier, J.; Basset, J.-M. Catalytic oxidation of light alkanes (C1-C4) by heteropoly compounds. *Chem. Rev.* **2014**, *114*, 981–1019. [CrossRef] [PubMed]
13. Min, J.-S.; Ishige, H.; Misono, M.; Mizuno, N. Low-temperature selective oxidation of methane into formic acid with H_2O_2 gas mixture catalyzed by bifunctional catalyst of palladium-heteropoly compound. *J. Catal.* **2001**, *198*, 116–121. [CrossRef]
14. Chen, L.; Yang, B.; Zhang, X.; Dong, W.; Zhang, X. Methane partial oxidation in liquid phase using vanadium-containing heteropolyacid catalysts in oleum. *Chin. J. Catal.* **2006**, *27*, 462–464.
15. Starokon, E.V.; Parfenov, M.V.; Arzumanov, S.S.; Pirutko, L.V.; Stepanov, A.G.; Panov, G.I. Oxidation of methane to methanol on the surface of FeZSM-5 zeolite. *J. Catal.* **2013**, *300*, 47–54. [CrossRef]
16. Parfenov, M.V.; Starokon, E.V.; Pirutko, L.V.; Panov, G.I. Quasicatalytic and catalytic oxidation of methane to methanol by nitrous oxide over FeZSM-5 zeolite. *J. Catal.* **2014**, *318*, 14–21. [CrossRef]
17. Xu, J.; Armstrong, R.D.; Shaw, G.; Dummer, N.F.; Freakley, S.J.; Taylor, S.H.; Hutchings, G.J. Continuous selective oxidation of methane to methanol over Cu- and Fe-modified ZSM-5 catalysts in a flow reactor. *Catal. Today* **2016**, *270*, 93–100. [CrossRef]
18. Dandu, N.K.; Reed, J.A.; Odoh, S.O. Performance of density functional theory for predicting methane-to-methanol conversion by a tri-copper complex. *J. Phys. Chem. C* **2018**, *122*, 1024–1036. [CrossRef]
19. Michalkiewicz, B.; Kałucki, K.; Sośnicki, J.G. Catalytic system containing metallic palladium in the process of methane partial oxidation. *J. Catal.* **2003**, *215*, 14–19. [CrossRef]
20. Xie, Y.; Gao, M.; Zhang, H.; Zeng, S.; Zhao, X.; Zhao, Y.; Su, H.; Song, J.; Li, X.; Jia, Q. Improvement role of CNTs on catalytic performance in the CeO_2/xCNTs-CuO catalysts. *Int. J. Hydrogen Energy* **2016**, *41*, 21979–21989. [CrossRef]
21. Shi, L.; Zhang, G.; Wang, Y. Tailoring catalytic performance of carbon nanotubes confined CuO CeO_2 catalysts for CO preferential oxidation. *Int. J. Hydrogen Energy* **2018**, *43*, 18211–18219. [CrossRef]
22. Tavasoli, A.; Anahid, S.; Nakhaeipour, A. Effects of confinement in carbon nanotubes on the performance and lifetime of Fischer-Tropsch iron nano catalysts. *Iran. J. Chem. Chem. Eng. Int. Engl. Ed.* **2010**, *29*, 1–12.

23. Sanders, T.; Papas, P.; Veser, G. Supported nanocomposite catalysts for high-temperature partial oxidation of methane. *Chem. Eng. J.* **2008**, *142*, 122–132. [CrossRef]
24. Song, Y.-M.; Wang, F.; Luo, S.-J.; Guo, R.-B.; Xu, D. Methane hydrate formation improved by water-soluble carbon nanotubes via π-π conjugated molecules functionalization. *Fuel* **2019**, *243*, 185–191. [CrossRef]
25. Irani, M.; Jacobson, A.T.; Gasem, K.A.; Fan, M. Modified carbon nanotubes/tetraethylenepentamine for CO_2 capture. *Fuel* **2017**, *206*, 10–18. [CrossRef]
26. Akbarzadeh, H.; Abbaspour, M.; Salemi, S.; Nazarian, A. Formation of methane clathrates in carbon nanotubes: A molecular dynamics study. *New J. Chem.* **2018**, *42*, 7083–7095. [CrossRef]
27. Liu, X.; Liu, J.; Chang, Z.; Sun, X.; Li, Y. Crystal plane effect of Fe_2O_3 with various morphologies on CO catalytic oxidation. *Catal. Commun.* **2011**, *12*, 530–534. [CrossRef]
28. Shahami, M.; Shantz, D.F. Zeolite acidity strongly influences hydrogen peroxide activation and oxygenate selectivity in the partial oxidation of methane over M,Fe-MFI (M: Ga, Al, B) zeolites. *Catal. Sci. Technol.* **2019**, *9*, 2945–2951. [CrossRef]
29. Taran, O.P.; Yashnik, S.A.; Boltenkov, V.V.; Parkhomchuk, E.V.; Sashkina, K.A.; Ayusheev, A.B.; Babushkin, D.E.; Parmon, V.N. Formic Acid Production Via Methane peroxide oxidation over oxalic acid activated Fe-MFI catalysts. *Top. Catal.* **2019**, *62*, 491–507. [CrossRef]
30. Chen, W.; Fan, Z.; Pan, X.; Bao, X. Effect of confinement in carbon nanotubes on the activity of Fischer−Tropsch iron catalyst. *J. Am. Chem. Soc.* **2008**, *130*, 9414–9419. [CrossRef] [PubMed]
31. Dong, B.; Han, Z.; Zhang, Y.; Yu, Y.; Kong, A.; Shan, Y. Origin of the ability of alpha-Fe_2O_3 mesopores to activate C-H bonds in methane. *Chem. A Eur. J.* **2016**, *22*, 2046–2050. [CrossRef] [PubMed]
32. Davico, G.E. The Conversion of Methane to Methanol: A Reaction Catalyzed by I^+ or I_2^+? *J. Phys. Chem. A* **2005**, *109*, 3433–3437. [CrossRef] [PubMed]
33. Xiao, Y.S.; Chen, L.Y.; Lu, R.X.; Tang, C.Q. Selective oxidation of methane to methanol with organic oxidants catalyzed by iodine in non-aqueous acetic acid medium. *Appl. Mech. Mater.* **2015**, *723*, 624–628. [CrossRef]